Cell Biology International ISSN 1065-6995
doi: 10.1002/cbin.10303

METHODOLOGY

Measuring mechanical properties in cells: three easy methods for biologists

Navid Bonakdar[1], Achim Schilling[1], Pablo Lennert[1], Marina Spörrer[1], Richard C. Gerum[1], José Luis Alonso[2] and Wolfgang H. Goldmann[1]*

1 Department of Physics, Biophysics, Friedrich-Alexander-University Erlangen-Nuremberg, Erlangen, Germany
2 Massachusetts General Hospital/Harvard Medical School, Charlestown, MA 02129, USA

Abstract

The mechanism by which cells sense stresses and transmit them throughout the cytoplasm and the cytoskeleton (CSK) and by which these mechanical signals are converted into biochemical signaling responses is not clear. Specifically, there is little direct experimental evidence on how intracellular CSK structural elements in living cells deform and transmit stresses in response to external mechanical forces. Existing theories have invoked various biophysical and biochemical mechanisms to explain how cells spread, deform, divide, move, and change shape in response to mechanical inputs, but rigorous tests in cells are lacking. The lack of data and understanding is preventing the identification of mechanisms and sites of mechano-regulation in cells. Here, we introduce and describe three unique and easy methods for biologists to determine mechanical properties and signaling events in cells.

Keywords: cell stretching; endothelial cells; keratinocytes; magnetic tweezer rheology; mouse fibroblasts; traction microscopy

Introduction

Biomechanical studies of single cells and cell populations have been of interest for some time and in recent years have experienced a rapid development (Wang et al., 1993; Ezzell et al., 1997; Mierke et al., 2008, 2010; Möhl et al., 2009, 2012; Faust et al., 2011; Lange et al., 2013). Measuring cell mechanical properties in the field of muscle physiology was at the forefront and contributed significantly to the current understanding of the mechanism of muscle contraction (Huxley, 1957; Ra et al., 1999). The dynamics and kinetics of biochemical reactions between the most important muscle contractile proteins, actin and myosin, has been determined with high accuracy and temporal resolution based on relatively simple measurements of force and length changes of the skeletal muscle (Hill, 1965). The regular, almost crystalline arrangement in the muscle contractile apparatus allows the use of simple mathematical models to interpret the measurements obtained macroscopically in relation to molecular processes (Huxley, 1957; Hill, 1965; Kawai and Brandt, 1980).

In non-muscle cells, however, the conditions are more complex. Their diverse mechanical function, including migration, division, phagocytosis, etc. are determined by actomyosin motors. Numerous other regulatory molecules and structure-forming proteins of the cytoskeleton are also significantly involved (Hartmann and Spudich, 2012). This is often augmented by time-varying, irregular network-like structures of the cytoskeleton. The assignment of mechanical measurements and biochemical processes in non-muscle cells are, therefore, unclear. A particular difficulty is the absence of macroscopic tissues containing the cells and that experiments have to be performed in vitro. In the following paragraphs, three novel methods for elucidating the mechanical properties of live cells are described, which can be easily applied in cell biological laboratories.

Methods for measuring mechanical cellular properties

Mechanical cell stretcher

In a typical stretching experiment, uniaxial cyclic stretch is applied (Faust et al., 2011; Bonakdar et al., 2012). The

*Corresponding author: e-mail: wgoldmann@biomed.uni-erlangen.de
Navid Bonakdar and Achim Schilling contributed equally to this work.

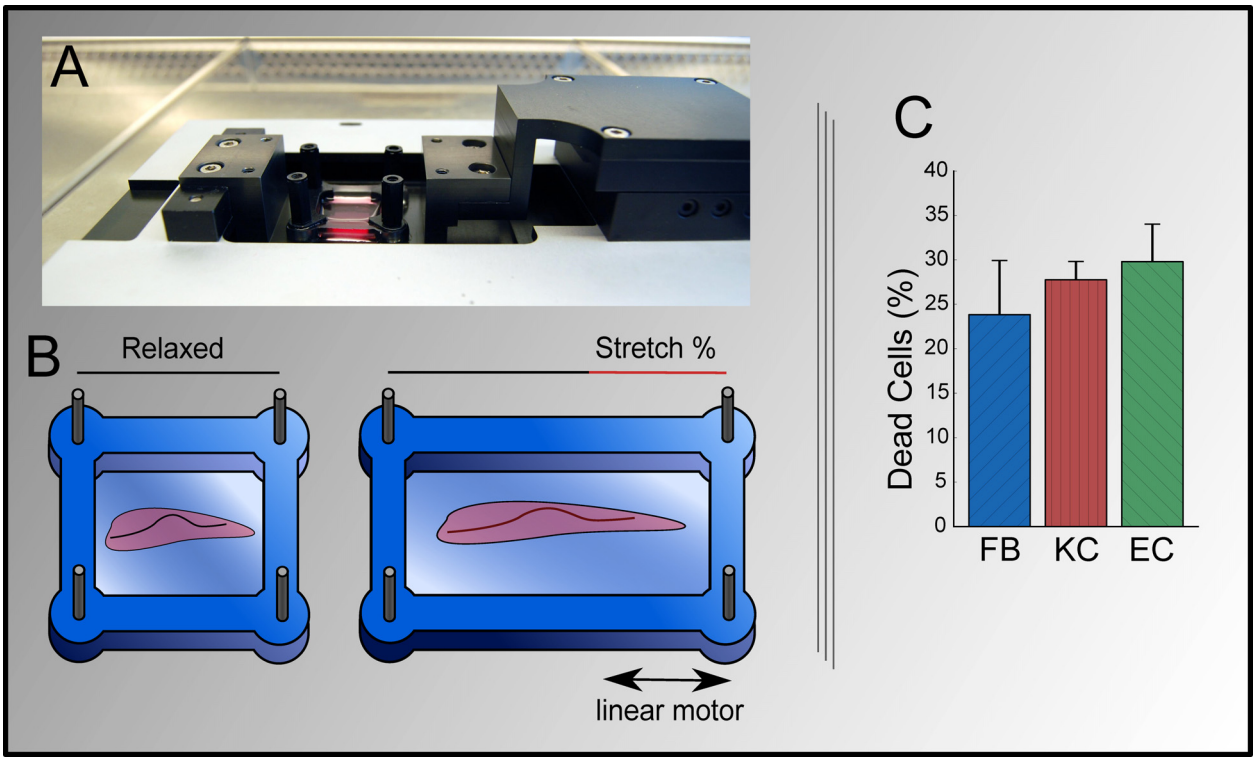

Figure 1 Mechanical cell stretcher. (A) A photographic view of the cell stretcher. (B) Cells are plated on an elastomeric PDMS-membrane coated with about 1 mg/mL of extracellular matrix proteins, fibronectin (fibroblasts, endothelial cells) or collagen-I (keratinocytes). The membrane is stretched up to 30% by a linear motor. (C) Data from stretch experiments. Membrane stretching at 30% and 0.25 Hz for 1 h significantly increased the number of dead (detached) cells for FB = fibroblasts, KC = kerationocytes, EC = endothelial cells. Error bars are given as standard error.

stretcher consists of a linear stage for uniaxial stretch and is driven by a computer-controlled stepper motor (Fig. 1A). Cells are plated on a flexible polydimethylsiloxan (PDMS) substrate that is molded into the shape of a cell culture well with 4.0 cm^2 internal surface and is kept in an incubator under normal cell culture conditions (37°C, 5% CO_2, 95% humidity) (Fig. 1B). The substrates are coated with extracellular matrix proteins in PBS overnight at 4°C, and normally 10,000 cells are seeded 24 h prior to experiments.

As in most stretch experiments, the vulnerability is defined by a viability test, which determines the ratio of dead to alive cells after the stretch is performed. This is done by taking randomly chosen positions on the substrate and counting the number of single cells within these positions before and after stretch. On the basis of life/dead-staining (calcein-AM/propidium iodide), the fraction of dead cells is determined (Tschumperlin and Margulies, 1998).

Sample experiments shown here give the response of mouse fibroblasts (FB), keratinocytes (KC), and endothelial cells (EC) to stretch (substrate/cell extension) in time-matched (1 h) experiments at 30% stretch. The percentage of dead cells at 0% stretch was between 3 and 4% for all cell lines. When 30% stretch is applied, an increase in cell vulnerability is observed of the following order: EC > KC > FB (Fig. 1C). Since the mechanical stress increases in direct proportion with cell stiffness and stretch amplitude (Hooke's law), the higher number of dead cells after stretch may be due to stretch-induced cell stress arising from higher internal prestress. To verify this, the magnetic tweezer device can be used.

Magnetic tweezer

The magnetic tweezer device has been described in detail (Alenghat et al., 2000; Kollmannsberger and Fabry, 2007). For measurements, normally 2×10^5 cells are seeded overnight into a 35 mm Ø tissue culture dish (Fig. 2A). Thirty minutes before the experiments, the cells are incubated with extracellular matrix protein-coated super-paramagnetic beads of 5 μm Ø (Fig. 2B). A magnetic field is generated using a solenoid with a needle-shaped core (HyMu80 alloy, Carpenter, Reading, PA). The needle tip is placed at a distance of 20–30 μm from a bead bound to the cell using a motorized micromanipulator (Fig. 2C). During measurements, bright-field images are taken by a CCD camera at a rate of 40 frames/s. The bead position is then

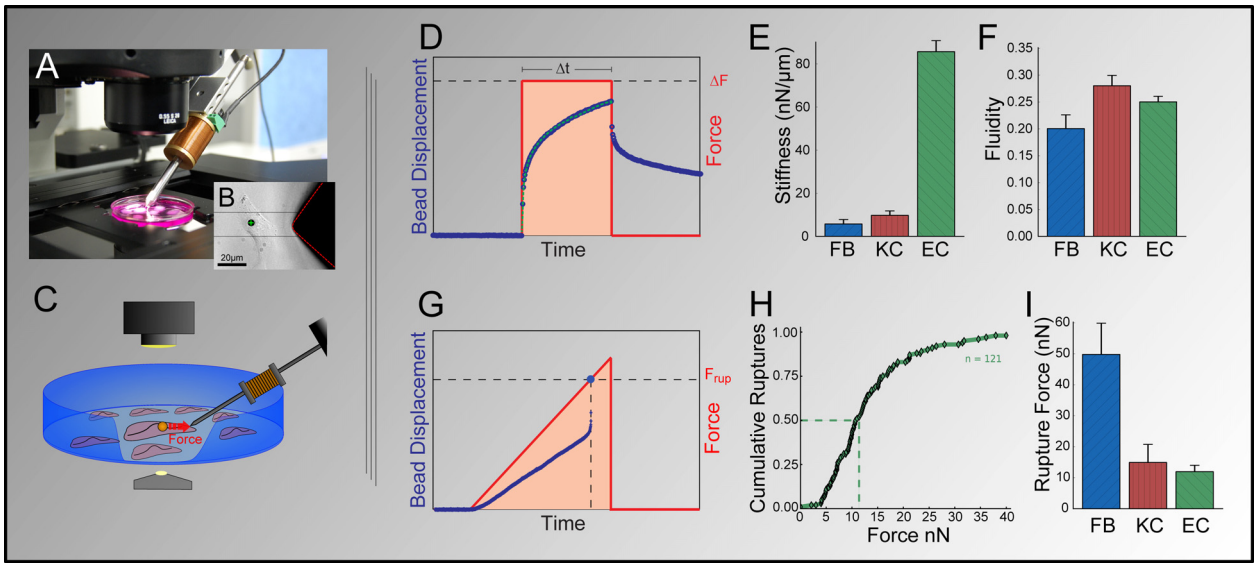

Figure 2 Magnetic tweezer setup. (A) Photographic image of the magnetic tweezer device. (B) Tweezer tip close to a magnetic bead attached to the cell (inset). (C) A high magnetic field gradient is generated by a needle-shaped high-permeability core of a solenoid attached to a micromanipulator. The gradient force generated by the magnetic tweezer acts on superparamagnetic beads coated with extracellular matrix proteins of 1 mg/mL fibronectin (fibroblasts, endothelial cells) or laminin-I (keratinocytes). Beads are bound to the cell surface via integrin receptors that connect the extracellular space with the intracellular cytoskeleton. (D) Creep protocol. Typical bead displacement (blue dots) in response to a single force step protocol (red line). The response was fitted by a power-law (white dashed line). (E) Results from stiffness measurements are of mean standard error: endothelial cells > keratinocytes > fibroblasts. (F) Cell fluidity, that is, cellular dynamics (β-value) with mean SE of endothelial cells, keratinocytes, and fibroblasts. (G) Ramp protocol. A force ramp was applied up to 40 nN (red line) and the force at which the rupture event occurs, was detected (blue dot). (H) Fraction of detached beads versus pulling force. The dashed line indicates the median rupture value for endothelial cells. (I) Median rupture force exerted from the cumulative rupture distribution (Note that due to fibronectin-coated beads on EC, the cells are less adhesive). Errors were determined by a bootstrap method.

tracked on-line using an intensity-weighted center-of-mass algorithm. Measurements on multiple beads per well are normally performed at 37°C for 30 min, using a heated microscope stage on an inverted microscope at 40× magnification (NA 0.6) under bright-field illumination.

Magnetic tweezer microrheometry measures the cell deformation in response to magnetically generated forces (Kollmannsberger and Fabry, 2011), which are excerted on extracellular matrix protein-coated superparamagnetic beads attached to integrins (Fig. 2C). A creep protocol (Fig. 2D) is applied, where the force is increased from zero to a fixed value (typically 10 nN) and held for some time (typically $t = 1$ s) and then sharply decreases back to zero again. The cell responds to this force application by a deformation, which follows a power law (Kollmannsberger and Fabry, 2007). This response can be described, using $J(t)=J_0 \cdot (\frac{t}{\tau_0})^{\beta}$, from which the cell stiffness $1/J_0$ and fluidity can be obtained. Figures 2E and 2F show results from mouse FB, KC, and EC. The stiffness $1/J_0$ is of the following order: EC > KC > FB. EC show about tenfold higher stiffness than FB and KC, indicating a higher baseline tension, since the total cytoskeletal prestress is the sum of baseline prestress and externally imposed stress (Kollmannsberger et al., 2011). The fluidity describes spring-like ($\beta = 0$) or dashpot-like ($\beta = 1$) cellular response and gives insight of dynamic processes of the cytoskeleton (Bursac et al., 2005).

To rule out that an increased number of detached cells during pull are the result of poor matrix adhesion, an increasing lateral force ramp protocol to integrin-coupled magnetic beads up to 80 nN is applied by a steel tip of the tweezer. This approach allows to record the force, at which the beads detach from the cells under certain bead-coating conditions and to estimate the adhesion strength (Fig. 2G). The force ramp up to 40 nN (green line) and the force, at which the rupture event occurs, was detected by the green dotted line for EC (Fig. 2H). The fraction of beads that detached from FB is lower than in KC and EC (Fig. 2I). Generally, when focal adhesion contacts of adherent cells are stimulated by external forces, they respond with restructuring and reinforcement of focal contacts, that is, focal adhesion strengthening (Choquet et al., 1997; Goldmann, 2002; Giannone et al., 2003; Deng et al., 2004). A controlled generation of such forces allows the study of dynamic processes in great detail.

Fourier transform traction microscopy

Adherent cells transfer forces onto the extracellular matrix. When cells are cultured on a polyacrylamide

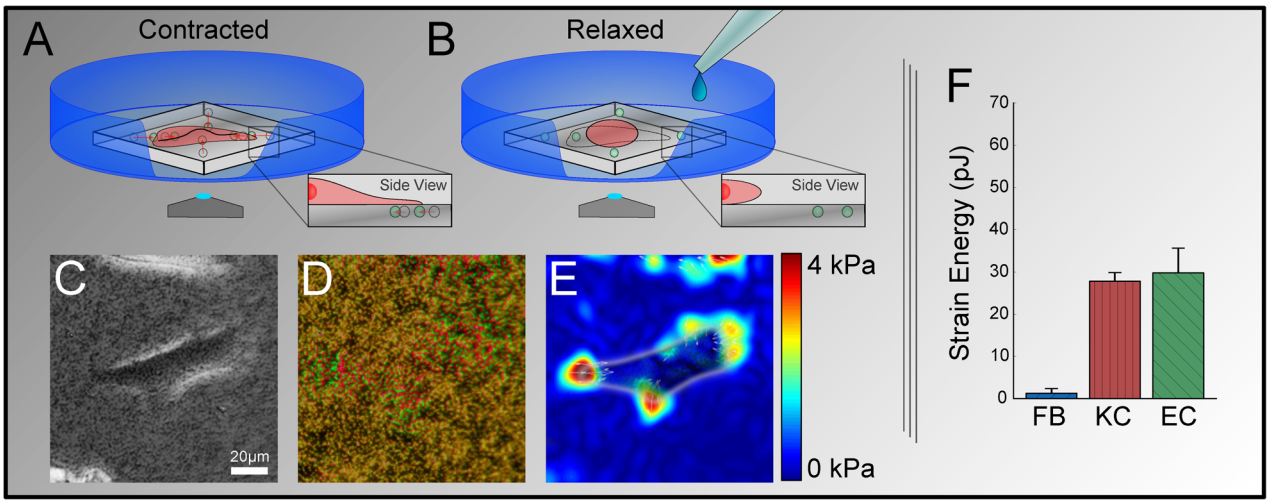

Figure 3 Traction force microscopy. (A) A schematic diagram of the setup. Fluorescent beads are embedded in a polyacrylamide gel. The gel surface is coated with extracellular matrix proteins of 1 mg/mL fibronectin (fibroblasts) or collagen-I (endothelial cells, keratinocytes). (B) The relaxed state of the cell is achieved by the addition of cytochalasin D and trypsin. (C–E) A bright field and fluorescent image (i.e., red indicates the contracted and green the relaxed states of the beads) as well as a traction image of a fibroblast. (F) Calculated strain energy normalized to the spreading area for FB = fibroblasts, KC = kerationocytes, EC = endothelial cells. Error bars indicate SE.

elastic substrate, in which fluorescent markers (e.g., 200 nm FluoSpheres) are embedded, forces can be made visible (Butler et al., 2002; Stamenovic et al., 2002, 2004; Deng et al., 2004). Depending on the elastic modulus of the elastic substrate and the contractile state of the cells, the fluorescent marker (bead) is displaced from the resting position. From the measured deformation of the elastic substrate, the size, orientation, and exact location of the force field below the cell can be reconstructed at sub-pixel precision using a Fourier-based algorithm (Butler et al., 2002). The elastic properties of the polyacrylamide substrate can be adjusted over a wide range (100 Pa to >50 kPa) by precisely varying the acrylamide/bisacrylamide cross-linker ratio and concentration. The surface of the polyacrylamide gel is activated with sulfosuccinimidyl 6 (4′-azido-2′-nitrophenyl-amino) hexanoate (sulfo-SANPAH) and then covalently coated with any extracellular matrix protein.

It has been possible to increase the resolution of the deformation field of the elastic matrix to 10 nm. In contrast to previous methods, for the calculation of the force field from traction microscopy, it is no longer necessary to know the exact location of the adhesive contacts or the outline of the cell (Dembo and Wang, 1999; Balaban et al., 2001; Butler et al., 2002). To obtain such additional information is time-consuming. This method allows the automatic calculation of the deformation and force field of the cell, which is free of potentially bias decisions of the researcher with a significantly higher throughput.

Here, traction measurements are performed on acrylamide/bisacrylamide gels (e.g., ratio 19:1 with a Young's modulus of 12.8 kPa and thickness of 300 μm) with 0.5 μm green fluorescent beads embedded at the top surface (Pelham and Wang, 1998; Raupach et al., 2007). Gels are then coated with extracellular matrix proteins at 4°C overnight. Cells are normally seeded on gels at a density between 10 and 20,000 cells in a 35 mm Ø tissue culture dish and incubated under normal growth conditions (Fig. 3A). During measurements, the cells are maintained at 37°C and 5% CO_2 in a humidified atmosphere of 95%. Cell tractions are computed with an unconstrained fast Fourier traction cytometry method (Butler et al., 2002) and measured before and after the cells are treated with a trypsin/cytochalasin D mix to relax the traction forces (Fig. 3B). Figures 3C–3E display the brightfield and fluorescence image as well a traction map of an adherent cell from which the strain energy is calculated (Fig. 3F).

The contractile forces (i.e., actomyosin apparatus) of spread cells are predominantly transmitted to the ECM as opposed to internal compression-bearing elements such as microtubules (Wang et al., 2002). Contractile forces of cells are characterized by the elastic strain energy stored in the ECM. The strain energy of EC is, under extracellular matrix conditions, slightly higher than KC, thus much higher (about tenfold) compared to FB (Fig. 3F). This finding supports observations of higher stiffness in KC and EC compared to FB that indicate higher cell motility.

Conclusions

Measurements provided here using different methods give direct mechanical evidence that the cytoskeleton has various functions in cells. Note that different extracellular matrix proteins used in the experiments described here activate different integrins which might result in slightly varying cellular adhesive forces. It remains, however, an open question in what way cellular cytoskeletal restructuring and reorganization processes are involved and trigger biomechanical signaling. Meanwhile, a number of laboratories have directed their research in elucidating the important aspect of signal transduction using some of these techniques. (For further reading, please refer to Eekhoff et al., 2011; Inoh et al., 2002; Naruse et al., 1998; Pullarkat et al., 2007; Takeda et al., 2006; Wang et al., 2005).

Acknowledgment and funding

We thank Astrid Mainka for her help. This work was supported in part by grants from Bayerische Forschungsallianz, Deutscher Akademischer Austauschdienst (DAAD), and Deutsche Forschungsgemeinschaft (DFG).

References

Alenghat FJ, Fabry B, Tsai KY, Goldmann WH, Ingber DE (2000) Analysis of cell mechanics in single vinculin-deficient cells using a magnetic tweezer. Biochem Biophys Res Commun 277: 93–9.

Balaban NQ, Schwarz US, Riveline D, Goichberg P, Tzur G, Sabanay I, Mahalu D, Safran S, Bershadsky A, Addadi L, Geiger B (2001) Force and focal adhesion assembly: a close relationship studied using elastic micropatterned substrates. Nat Cell Biol 3: 466–72.

Bonakdar NJL, Lautscham L, Czonstke M, Koch TM, Mainka A, Jungbauer T, Goldmann WH, Schroeder R, Fabry B (2012) Biomechanical characterization of a desminopathy in primary human myoblasts. Biochem Biophys Res Commun 419: 703–7.

Bursac P, Lenormand G, Fabry B, Oliver M, Weitz DA, Viasnoff V, Butler JP, Fredberg JJ (2005) Cytoskeletal remodelling and slow dynamics in the living cell. Nat Mater 4: 557–61.

Butler JP, Tolic-Norrelykke IM, Fabry B, Fredberg JJ (2002) Traction fields, moments, and strain energy that cells exert on their surroundings. Am J Physiol Cell Physiol 282: C595–605.

Choquet D, Felsenfeld DP, Sheetz MP (1997) Extracellular matrix rigidity causes strengthening of integrin-cytoskeleton linkages. Cell 88: 39–48.

Dembo M, Wang YL (1999) Stresses at the cell-to-substrate interface during locomotion of fibroblasts. Biophys J 76: 2307–16.

Deng L, Fairbank NJ, Fabry B, Smith PG, Maksym GN (2004) Localized mechanical stress induces time-dependent actin cytoskeletal remodeling and stiffening in cultured airway smooth muscle cells.. Am J Physiol Cell Physiol 287: C440–8.

Eekhoff A, Bonakdar N, Alonso JL, Hoffmann B, Goldmann WH (2011) Glomerular podocytes: a study of mechanical properties and mechano-chemical signaling. Biochem Biophys Res Commun 406: 229–33.

Ezzell RM, Goldmann WH, Wang N, Parasharama N, Ingber DE (1997) Vinculin promotes cell spreading by mechanically coupling integrins to the cytoskeleton. Exp Cell Res 231: 14–26.

Faust U, Hampe N, Rubner W, Kirchgessner N, Safran S, Hoffmann B, Merkel R (2011) Cyclic stress at mHz frequencies aligns fibroblasts in direction of zero strain. PloS ONE 6: e28963.

Giannone G, Jiang G, Sutton DH, Critchley DR, Sheetz MP (2003) Talin1 is critical for force-dependent reinforcement of initial integrin-cytoskeleton bonds but not tyrosine kinase activation. J Cell Biol 163: 409–19.

Goldmann WH (2002) Mechanical aspects of cell shape regulation and signaling. Cell Biol Int 26: 313–7.

Hartmann MA, Spudich JA (2012) The myosin superfamily at a glance. J Cell Sci 125: 1627–32.

Hill AV (1965) *Trails and trials in physiology*. London: E. Arnold, pp. 14–5.

Huxley AF (1957) Muscle structure and theories of contraction. Prog Biophys Biophys Chem 7: 255–318.

Inoh H, Ishiguro N, Sawazaki S, Amma H, Miyazu M, Iwata H, Sokabe M, Naruse K (2002) Uni-axial cyclic stretch induces the activation of transcription factor nuclear factor kappaB in human fibroblast cells. FASEB J 16: 405–7.

Kawai M, Brandt PW (1980) Sinusoidal analysis: a high resolution method for correlating biochemical reactions with physiological processes in activated skeletal muscles of rabbit, frog and crayfish. J Muscle Res Cell Motil 1: 279–303.

Kollmannsberger P, Fabry B (2007) High-force magnetic tweezers with force feedback for biological applications. Rev Sci Instrum 78: 114301-1-6.

Kollmannsberger P, Fabry B (2011) Linear and nonlinear rheology of living cells. Annu Rev Mater Res 41: 75–97.

Kollmannsberger P, Mierke CT, Fabry B (2011) Nonlinear viscoelasticity of adherent cells is controlled by cytoskeletal tension. Soft Matter 7: 3127–32.

Lange J, Auernheimer V, Strissel PL, Goldmann WH (2013) Influence of focal adhesion kinase on the mechanical behavior of cell populations. Biochem Biophys Res Commun 436:246–51.

Mierke CT, Kollmannsberger P, Paranhos-Zitterbart D, Smith J, Fabry B, Goldmann WH (2008) Mechano-coupling and regulation of contractility by the vinculin tail domain. Biophys J 94: 661–70.

Mierke CT, Kollmannsberger P, Zitterbart DP, Diez G, Koch TM, Marg S, Ziegler WH, Goldmann WH, Fabry B (2010) Vinculin facilitates cell invasion into three-dimensional collagen matrices. J Biol Chem 285: 13121–30.

Möhl C, Kirchgessner N, Schäfer C, Küpper K, Born S, Diez G, Goldmann WH, Merkel R, Hoffmann B (2009) Becoming stable and strong: The interplay between vinculin exchange dynamics and adhesion strength during adhesion site maturation. Cell Motil Cytoskeleton 66: 350–64.

Möhl C, Kirchgessner N, Schäfer C, Hoffmann B, Merkel R (2012) Quantitative mapping of averaged focal adhesion dynamics in migrating cells by shape normalization. J Cell Sci 125: 155–65.

Naruse K, Yamada T, Sokabe M (1998) Involvement of SA channels in orienting response of cultured endothelial cells to cyclic stretch. Am J Physiol 274: H1532–8.

Pelham RJ, Jr., Wang YL (1998) Cell locomotion and focal adhesions are regulated by the mechanical properties of the substrate. Biol Bull 194: 348–9; discussion 9–50.

Pullarkat PA, Fernández PA Ott A (2007) Rheological properties of the eukaryotic cell cytoskeleton. Phys Rep 449: 29–53.

Ra HJ, Picart C, Feng H, Sweeney HL, Discher DE (1999) Muscle cell peeling from micropatterned collagen: direct probing of focal and molecular properties of matrix adhesion. J Cell Sci 10: 1425–36.

Raupach C, Zitterbart DP, Mierke CT, Metzner C, Muller FA, Fabry B (2007) Stress fluctuations and motion of cytoskeletal-bound markers. Phys Rev E 76: 011918.

Stamenovic D, Mijailovich SM, Tolic-Norrelykke IM, Chen J, Wang N (2002) Cell prestress. II. Contribution of microtubules. Am J Physiol Cell Physiol 282: C617–24.

Stamenovic D, Suki B, Fabry B, Wang N, Fredberg JJ (2004) Rheology of airway smooth muscle cells is associated with cytoskeletal contractile stress. J Appl Physiol 96: 1600–5.

Takeda H, Komori K, Nishikimi N, Nimura Y, Sokabe M, Naruse K (2006) Bi-phasic activation of eNOS in response to uni-axial cyclic stretch is mediated by differential mechanisms in BAECs. Life Sci 79: 233–9.

Tschumperlin DJ, Margulies SS (1998) Equibiaxial deformation-induced injury of alveolar epithelial cells in vitro. Am J Physiol 275: L1173–83.

Wang N, Butler JP, Ingber DE (1993) Mechanotransduction across the cell surface and through the cytoskeleton. Science 260: 1124–7.

Wang N, Tolic-Norrelykke IM, Chen J, Mijailovich SM, Butler JP, Fredberg JJ, Stamenović D (2002) Cell prestress. I. Stiffness and prestress are closely associated in adherent contractile cells. Am J Physiol Cell Physiol 282: C606–16.

Wang JG, Miyazu M, Xiang P, Li SN, Sokabe M, Naruse K (2005) Stretch-induced cell proliferation is mediated by FAK-MAPK pathway. Life Sci 76: 2817–25.

Received 10 December 2013; accepted 14 April 2014.
Final version published online 19 June 2014.